European Journal of Pharmaceutics and Biopharmaceutics 71 (2009) 214–222

Contents lists available at ScienceDirect

European Journal of Pharmaceutics and Biopharmaceutics

journal homepage: www.elsevier.com/locate/ejpb

Research paper

Nanoparticle-mediated combination chemotherapy and photodynamic therapy overcomes tumor drug resistance *in vitro*

Ayman Khdair [a,b], Hitesh Handa [c], Guangzhao Mao [c], Jayanth Panyam [b,*]

[a] Department of Pharmaceutical Sciences, Wayne State University, Detroit, MI, USA
[b] Department of Pharmaceutics, University of Minnesota, Minneapolis, MN, USA
[c] Department of Chemical Engineering and Materials Science, Wayne State University, Detroit, MI, USA

ARTICLE INFO

Article history:
Received 5 May 2008
Accepted in revised form 19 August 2008
Available online 29 August 2008

Keywords:
Nanoparticles
Photodynamic therapy
Nuclear delivery
Drug efflux
Reactive oxygen species
Photosensitizer
Cellular delivery
Cytotoxicity

ABSTRACT

Drug resistance limits the success of many anticancer drugs. Reduced accumulation of the drug at its intracellular site of action because of overexpression of efflux transporters such as P-glycoprotein (P-gp) is a major mechanism of drug resistance. In this study, we investigated whether photodynamic therapy (PDT) using methylene blue, also a P-gp inhibitor, can be used to enhance doxorubicin-induced cytotoxicity in drug-resistant tumor cells. Aerosol OT (AOT)-alginate nanoparticles were used as a carrier for the simultaneous cellular delivery of doxorubicin and methylene blue. Methylene blue was photoactivated using light of 665 nm wavelength. Induction of apoptosis and necrosis following treatment with combination chemotherapy and PDT was investigated in drug-resistant NCI/ADR-RES cells using flow cytometry and fluorescence microscopy. Effect of encapsulation in nanoparticles on the intracellular accumulation of doxorubicin and methylene blue was investigated qualitatively using fluorescence microscopy and was quantitated using HPLC. Encapsulation in AOT-alginate nanoparticles significantly enhanced the cytotoxicity of combination therapy in resistant tumor cells. Nanoparticle-mediated combination therapy resulted in a significant induction of both apoptosis and necrosis. Improvement in cytotoxicity could be correlated with enhanced intracellular and nuclear delivery of the two drugs. Further, nanoparticle-mediated combination therapy resulted in significantly elevated reactive oxygen species (ROS) production compared to single drug treatment. In conclusion, nanoparticle-mediated combination chemotherapy and PDT using doxorubicin and methylene blue was able to overcome resistance mechanisms and resulted in improved cytotoxicity in drug-resistant tumor cells.

1. Introduction

Development of drug resistance is a major impediment to the success of anticancer chemotherapy. It is estimated that up to 500,000 new cases of cancer patients each year will develop drug-resistant phenotype [1]. Tumor cells utilize multiple mechanisms to reduce the accumulation of the anticancer drug at its intracellular site of action. Overexpression of P-glycoprotein (P-gp), a drug efflux transporter, is an important determinant of tumor drug resistance [2]. In addition, the efficacy of drugs such as doxorubicin is compromised by acidic tumor microenvironment and by sequestration in acidic intracellular organelles such as lysosomes [3,4]. Thus, therapies that target multiple mechanisms of resistance may be needed to effectively overcome tumor drug resistance.

Photodynamic therapy (PDT) has emerged as a popular adjuvant therapy for cancer and has been approved as a primary treatment option for certain neoplastic conditions including inoperable esophageal tumors, head and neck cancers, and microinvasive endo-bronchial non-small cell lung carcinoma [5,6]. PDT is also being investigated in preclinical and clinical studies for other cancer types including breast, prostate and ovarian. In PDT, a light-activated photosensitizer generates singlet oxygen ($^1O_2$) and other reactive oxygen species (ROS), which result in tumor cell kill [5,7,8].

Recent studies indicate that photosensitizers such as methylene blue may also be able to inhibit P-gp mediated drug efflux [9]. While the mechanism is not clearly understood, P-gp inhibition was independent of the photodynamic activity. Also, studies suggest that simultaneous PDT and chemotherapy can release the sequestered drug from acidic compartments, and thereby increase drug's availability at its intracellular site of action [10,11]. Based on these properties, we rationalized that methylene blue-mediated PDT has the potential to enhance the cytotoxicity of P-gp substrates such as doxorubicin in resistant tumor cells.

* Corresponding author. Department of Pharmaceutics, College of Pharmacy, Masonic Cancer Center, University of Minnesota, 308 Harvard st. SE., Minneapolis, MN 55455, USA. Tel.: +1 612 624 0951; fax: +1 612 626 2251.
E-mail address: jpanyam@umn.edu (J. Panyam).

0939-6411/$ - see front matter © 2008 Elsevier B.V. All rights reserved.
doi:10.1016/j.ejpb.2008.08.017

To be able to achieve effective enhancement, however, both the photosensitizer and the anticancer drug need to be colocalized in the tumor cell. One approach to achieving colocalization is to deliver both the photosensitizer and the anticancer drug simultaneously to the tumor cell using a delivery system that encapsulates both agents. Several nanoparticulate systems have been investigated for the delivery of photosensitizers [12–14] and chemotherapeutic agents [15–17] to tumor cells. We have recently reported a novel surfactant-polymer nanoparticle system, formulated using Aerosol OT™ (docusate sodium; AOT) and alginate, for efficient encapsulation and sustained cellular delivery of polar, weak bases like methylene blue and doxorubicin [18]. AOT is an anionic, double-tailed surfactant used as an oral, topical and intramuscular excipient [19]. Alginate is a polysaccharide polymer obtained from sea weeds and is used extensively in drug delivery and tissue engineering applications [20,21]. In this study, we investigated AOT-alginate nanoparticles for combination chemotherapy and PDT in drug-resistant tumors cells. Our studies show that nanoparticle-mediated combination therapy significantly increases the drug accumulation in drug-resistant tumor cells and effectively overcomes tumor drug resistance.

2. Materials and methods

2.1. Materials

Methylene blue, doxorubicin, sodium alginate, polyvinyl alcohol, ammonium acetate, and calcium chloride were purchased from Sigma–Aldrich (St. Louis, MO). AOT, verapamil, acetonitrile, methanol, and methylene chloride were purchased from Fisher Scientific (Chicago, IL). NCI/ADR-RES cells were obtained from the National Cancer Institute. Propidium iodide, ribonuclease A, and Triton X-100 were purchased from Roche Diagnostics Corporation (Indianapolis, IN). MTS assay kit (CellTiter 96® AQ_{ueous}), trypsin-like enzyme (TryplE®), 5-(and-6)-chloromethyl-2′,7′-dichlorodihydrofluorescein diacetate acetyl ester (CM-H_2DCFDA), and phosphate buffered saline (PBS) were purchased from Invitrogen (Carlsbad, CA).

2.2. Methods

2.2.1. Nanoparticle formulation

AOT-alginate nanoparticles loaded with both doxorubicin and methylene blue were formulated using a multiple emulsification cross-linking method developed in our laboratory [22]. In a typical procedure, aqueous solution of sodium alginate (1% w/v; 1 ml) containing methylene blue (5 mg) and doxorubicin (5 mg) was emulsified into AOT solution in methylene chloride (2.5% w/v; 2 ml) by sonication for 1 min over an ice bath (Sonicator 3000™, Misonix, Farmingdale, NY). The water-in-oil emulsion was further emulsified into 15 ml of an aqueous solution of polyvinyl alcohol (average MW 30,000–70,000; 2% w/v) to form water-in-oil-in-water emulsion. While stirring, 5 ml of aqueous calcium chloride solution (60% w/v) was gradually added to the final emulsion. Methylene chloride was evaporated by stirring at ambient conditions for 18 h and then under vacuum for 1 h. To remove free doxorubicin and methylene blue and excess polyvinyl alcohol, nanoparticles suspension was subjected to ultracentrifugation (145,000*g* for 30 min, Beckman, Palo Alta, CA) thrice and resuspended in between in deionized water. Aggregates were removed by centrifugation of the nanoparticle suspension at 1000 rpm for 3 min (Eppendorf® 5810 R, Eppendorf, Westbury, NY). The nanoparticle suspension in deionized water was lyophilized (FreeZone 4.5®, Labconco, Kansas City, MO) following the final centrifugation step.

2.2.2. Nanoparticle characterization

Nanoparticles were characterized for morphology and size using atomic force microscopy (AFM). Nanoparticles suspended in deionized water (100 μg/ml) were spread over a polyethyleneimine-coated glass coverslip and then air dried. Nanoparticles were then imaged using Nanoscope III (Digital Instruments/VEECO, Santa Barbara, CA) with an E scanner probe in the tapping mode. Particle size was determined by calculating the number-average diameter of at least 50 nanoparticles in 10 different fields. Particle size was further confirmed using dynamic light scattering. About 1 mg of nanoparticles was suspended in 10 ml deionized water by sonication and subjected to particle size analysis (90Plus®, Brookhaven Instruments, Holtsville, NY). Data were analyzed by a non-negatively constrained least squares algorithm using 90Plus®.

Surface charge of nanoparticles was determined by measuring zeta potential using electrophoretic light scattering. Briefly, 1 mg of nanoparticles was suspended in 1 ml deionized water and subjected to zeta potential analysis using a zeta-sizer (90Plus®).

To determine drug loading in nanoparticles, about 5 mg of nanoparticles was extracted with 10 ml methanol for 2 h in dark and then centrifuged for 10 min at 13,000 rpm. The supernatant was analyzed for doxorubicin and methylene blue concentrations using a Beckman Coulter HPLC system (Fullerton, CA) equipped with System Gold® 125 solvent module and System Gold® 508 auto-injector. Synergi™ Polar-RP column (4.6 × 150 mm ODS and 4 μm particle size, Phenomenex, Torrance, CA), UV detection at 598 nm absorbance wavelength (System Gold® 168 PDA UV/vis detector, Beckman), and fluorescence detection at excitation and emission wavelengths of 505 and 550 nm (FP-2020 plus fluorescence detector; JASCO Inc., Easton, MD) were used. Mobile phase consisting of acetonitrile and ammonium acetate (10 mM; adjusted to pH 4 with glacial acetic acid) at (78:22) ratio and a flow rate of 1 ml/min was used. Retention time was ∼4.5 and ∼9.5 min for doxorubicin and methylene blue, respectively. Drug loading in nanoparticles was defined as w/w percentage of methylene blue or doxorubicin in 100 mg of nanoparticles.

2.2.3. In vitro release studies

Doxorubicin and methylene blue release from nanoparticles was determined in RPMI cell culture medium without phenol red and serum. Nanoparticle suspension (1 mg/1 ml) was placed in 1.5 ml Eppendorf® tubes in an incubator shaker (Brunswick Scientific, C24 incubator shaker, NJ) set at 100 rpm and 37 °C. At predetermined time intervals, nanoparticle suspension was centrifuged for 20 min at 20,000*g* and the supernatant was lyophilized. Doxorubicin and methylene blue in the lyophile were extracted with 1 ml methanol (Labquake™ shaker, Barnstead Thermolyne, Dubuque, IA) for 3 h in dark at room temperature. Methanolic extract was then centrifuged for 20 min at 20,000*g*. Doxorubicin and methylene blue concentrations in the supernatant were determined by HPLC. Degradation rates of doxorubicin and methylene blue under the release conditions were determined and were used to correct the *in vitro* release of the two drugs.

2.2.4. Cytotoxicity studies

NCI/ADR-RES cells grown at 37 °C and 5% CO_2 in RPMI 1640 media were cultured for 24 h in 96-well plates at a cell density of 5000/well/0.1 ml. Medium was then removed and cells were incubated with fresh medium containing 0.5 μM doxorubicin and 0.6 μM methylene blue in nanoparticles (equivalent to 3.3 μg/ml of nanoparticles) or in solution for 24 h. The dose of doxorubicin and methylene blue was chosen based on published IC_{50} values and initial dose optimization studies. Treatments were then removed, cells were washed twice with PBS and fresh medium was added. Cells were then exposed to a light dose of 2400 mJ/cm^2 at 665 nm wavelength (LumaCare™ LC-122M). About 24 h following

light exposure, cell viability was determined using MTS assay. Untreated cells, and cells that received an equivalent amount of empty nanoparticles, methylene blue and doxorubicin in solution, either drug in solution or encapsulated in nanoparticles along with equivalent dose of light were used as control groups. Cells that received same treatments as above but without light exposure were used as dark controls.

To study the induction of necrosis and apoptosis following PDT, a flow cytometry-based annexin-V FITC/propidium iodide assay was used. Annexin-V binds with high affinity to phosphatidylserine, which translocates to the outer leaflet of plasma membrane in the early stages of apoptosis. Propidium iodide (PI) stains DNA in cells that have lost membrane integrity including those undergoing necrosis and those in late stages of apoptosis. Briefly, NCI/ADR-RES cells were cultured in 35 mm petri dishes (500,000 cells/1 ml) for 24 h. Following treatment with a combination of doxorubicin and methylene blue, free or encapsulated in nanoparticles, for 24 h, cells were washed twice with PBS and exposed to a light dose of 2400 mJ/cm^2. Cells were then incubated for 3, 12 or 24 h at 37 °C, trypsinized and then centrifuged at 600*g* for 6 min. Collected cells were stained with FITC-conjugated annexin-V and PI according to manufacturer's instructions (BD Pharmingen®, San Jose, CA) and then immediately analyzed using a flow cytometer (FACSCalibur™, BD). FITC and PI fluorescence emissions were detected in FL-1 (530/30 nm) and FL-2 (585/42 nm) modes, respectively. Data from at least 20,000 cells were analyzed using CellQuest® (BD) and FlowJo® software (Tree Star, Ashland, OR). Apoptosis or necrosis was calculated based on the percent of total cells counted in each sample that stained positive for annexin-V or PI, respectively.

Induction of necrosis was further verified using fluorescence microscopy. Cells were seeded in 6-well plates (500,000 cells/well/1 ml) for 24 h. Following treatment with medium containing 0.5 μM doxorubicin and 0.6 μM methylene blue in nanoparticles or in solution for 24 h, cells were washed twice with PBS and exposed to a light dose of 2400 mJ/cm^2. Cells were then incubated for 24 h at 37 °C, and then treated with 10 μM PI for 3 h at 37 °C. Cells were then washed twice with PBS and cell images were acquired every 15 min with an inverted fluorescence microscope (Axiovert 40CFL, Carl Zeiss MicroImaging, Inc., Thornwood, NY), equipped with a mercury lamp and a digital camera (ProgRes® C3, JENOPTIK Laser, Jena, Germany). Images were captured in phase contrast mode and using a Cy3 filter (λ_{ex} and λ_{em} of 535/50 and 590–700 nm, respectively) to detect PI-associated red fluorescence.

2.2.5. Cell cycle analysis

To study the effect of combination therapy on cell cycle, Telford's assay was used. Cells were cultured in 35 mm petri dishes (500,000 cells/1 ml) for 24 h. Cells were then treated as described for cytotoxicity assays. Cells were then incubated for 3 or 36 h at 37 °C, trypsinized and centrifuged at 600*g* for 6 min. The cell pellet was resuspended in 1.0 ml of Telford's reagent [16.8 mg of EDTA disodium salt, 13.4 mg of ribonuclease A (93 U/mg), 25 mg of propidium iodide, and 0.5 ml of Triton X-100 in 500 ml of PBS]. Cellular DNA content stained with PI was analyzed using flow cytometry.

2.2.6. Cellular accumulation of doxorubicin

Cells were grown in 24-well plates at 50,000/well/ml cell density for 48 h. Cells were then incubated with 2.0 μM doxorubicin and 2.7 μM methylene blue in solution or encapsulated in nanoparticles (equivalent to 13.2 μg/ml nanoparticles). After 2 h, treatments were removed and cells were washed twice with PBS. Cells were then incubated with 300 μl/well cell lysis buffer (1% Triton X-100 in 0.1 M phosphate buffer, pH 6.5) in an orbital shaker for 1 h at 100 rpm and 37 °C. After complete cell lysis, protein content in the cell lysate was determined using BCA protein assay according to the manufacturer's instructions (Peirce, Rockford, IL). Doxorubicin in the cell lysate was extracted with 0.5 ml methanol for 2 h in dark at room temperature. Concentration of doxorubicin in the methanolic extract was determined using HPLC. Drug concentration in the cell lysate was normalized to the total cellular protein concentration. Cells treated with an equivalent dose of free or nanoparticle-encapsulated doxorubicin were used as controls. To study the effect of P-glycoprotein (P-gp) on cellular accumulation of doxorubicin, verapamil, a P-gp inhibitor, was used. Cells were treated with an equivalent dose of free or nanoparticle-encapsulated doxorubicin in the presence of 100 μM verapamil.

2.2.7. Intracellular distribution of doxorubicin and methylene blue

Cells were cultured in chamber slides (Nunc Lab-Tek II CC2 Chamber Slide System; Nalge Nunc International, Rochester, NY) at 200,000 cells/chamber cell density for 24 h. Cells were incubated with 6.7 μM methylene blue and 5.0 μM doxorubicin in solution or encapsulated in nanoparticles (equivalent to 33 μg/ml of nanoparticles). After 2 h, cells were incubated with 75 nM Lysotracker Green® for additional 30 min. Cells were then washed twice with PBS and incubated with 4′,6-diamidino-2-phenylindole (DAPI) for 10 min. Cells were washed twice with PBS and cell images were acquired using an Axiovert 40CFL fluorescence microscope. Images captured using Cy3 (for doxorubicin) and Cy5 (for methylene blue) filters were overlaid with those captured using FITC and DAPI filters to determine the localization of doxorubicin/methylene blue in lysosomes and nucleus, respectively.

In addition to microscopic analysis, intracellular distribution of doxorubicin was also quantified. Cells were grown in 6-well plates (500,000 cell/well/ml) for 48 h. Cells were incubated with 5.0 μM doxorubicin and 6.7 μM methylene blue in solution or encapsulated in nanoparticles for 2 h and then washed twice with PBS to remove any adherent nanoparticles. Cells were then trypsinized and centrifuged for 6 min at 100*g*. Cell pellet was collected and separated into cytosol and nuclear fractions using Nuclear/Cytosol fractionation kit according to manufacturer's instructions (BioVision, Mountain View, CA). The protein content of each fraction was quantified using BCA protein assay. Doxorubicin was extracted from nuclear and cytosol fractions for 5 h in dark at room temperature with 0.3 and 0.5 ml methanol, respectively. Doxorubicin concentration in the methanolic extract was determined using HPLC. Doxorubicin concentration in the nuclear/cytosol extracts was normalized to the protein concentration of the corresponding fraction.

2.2.8. Intracellular ROS generation

Intracellular ROS generation was studied using CM-H_2DCFDA ester. CM-H_2DCFDA is a derivative of reduced fluorescein that is used as a cell-permeant indicator of ROS. In the presence of ROS, CM-H_2DCFDA is converted to fluorescein. Cells were cultured for 48 h in 35 mm culture dishes at 200,000 cell/well/1 ml density. Cells were incubated with 0.5 μM doxorubicin and 0.6 μM methylene blue, free or encapsulated in nanoparticles, for 24 h. Cells were then washed with PBS and incubated with 5 μM CM-H_2DCFDA for 1 h. Cells were then exposed to light (2400 mJ/cm^2). Cell images were captured in phase contrast and epi-fluorescence modes (FITC filter) every 20 min for the first 3 h.

3. Results

3.1. Nanoparticle characterization

AFM studies indicated that nanoparticles had a spherical morphology, with an average diameter of 39 ± 7 nm determined by measuring the lateral width of particles (Fig. 1). Dynamic light

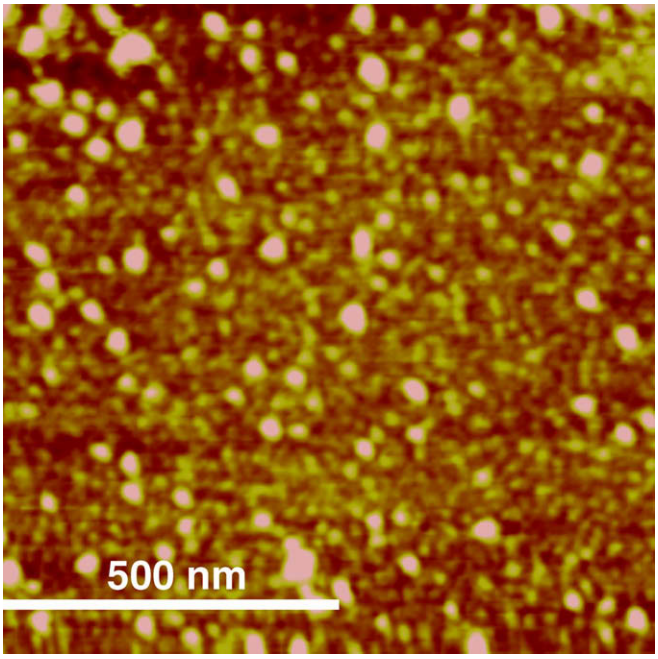

Fig. 1. AFM image of nanoparticles loaded with doxorubicin and methylene blue in the tapping mode in air. The image is a height image of a representative sample spot.

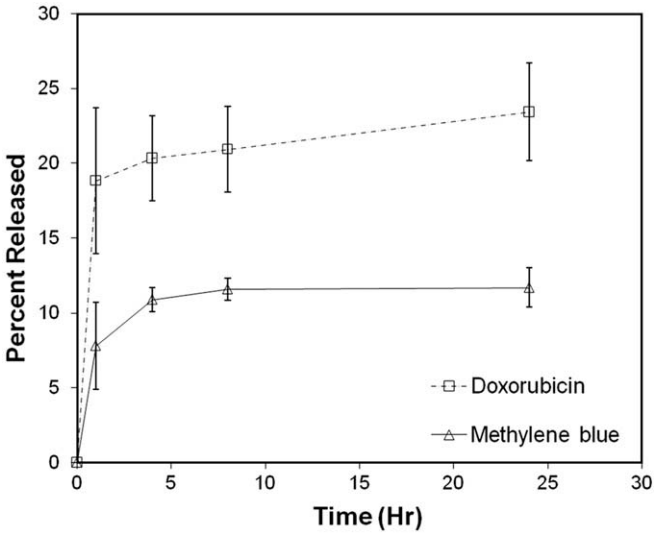

Fig. 2. *In vitro* release of doxorubicin and methylene blue from nanoparticles loaded with both drugs in culture medium. Nanoparticles were suspended in culture medium and then incubated at 37 °C and 100 rpm. Concentration of released doxorubicin and methylene blue was determined using HPLC. Data as mean ± SD (n = 3).

scattering (DLS) studies indicated a number-average diameter of 62 nm. The minor difference in particle size as measured by AFM and DLS studies could be explained by the fact that DLS measures effective hydrodynamic diameter of particles in hydrated state while AFM measures the diameter of dry particles. Electrophoretic light scattering measurements indicated that nanoparticles had a net negative surface charge of −25.1 ± 1.0 mV. Methylene blue and doxorubicin were efficiently encapsulated in nanoparticles; an average loading of 7.5 ± 0.1% w/w (69% encapsulation efficiency) and 7.2 ± 0.1% w/w (66% encapsulation efficiency) was obtained for methylene blue and doxorubicin, respectively.

3.2. In vitro release of doxorubicin and methylene blue

An initial burst release of the encapsulated doxorubicin and methylene blue was observed at the end of 1 h (∼19% and 8%, respectively, Fig. 2). The total release over 24 h was 23% and 12% for doxorubicin and methylene blue, respectively.

3.3. Tumor cell kill

Encapsulation of both drugs in nanoparticles along with light exposure significantly enhanced the tumor cell kill ($P < 0.05$; ∼75% cell kill compared to untreated controls, ANOVA, Fig. 3). Exposure of cells to light following treatment with doxorubicin and methylene blue in solution also resulted in significant cytotoxicity ($P < 0.05$), which, however, was less than that observed with nanoparticle-encapsulated drugs. Compared to vehicle or empty nanoparticle treatment, treatment with methylene blue in nanoparticles also induced significant cytotoxicity, but was less effective than the combination therapy. Treatment with methylene blue and doxorubicin without light exposure also resulted in significant cell killing ($P < 0.05$), suggesting that methylene blue could enhance the efficacy of doxorubicin in resistant tumor cells independent of its photosensitization activity. Treatment with free or nanoparticle-encapsulated doxorubicin did not significantly affect the cell viability. Similarly, empty nanoparticles or just light exposure alone had no effect on cell viability.

We also evaluated the mode of cell death following combination therapy using a flow cytometry-based assay. We determined the induction of apoptosis and necrosis at different time points following light exposure and found that the maximal difference between the treatment groups was observed at 12 h. As can be seen from Table 1, methylene blue doxorubicin nanoparticles resulted in a significant increase in the fraction of apoptotic and necrotic cells at the end of 12 h (data for 3 and 24 h not shown). Similar to that observed in the MTS-based cytotoxicity assay, combination therapy in the absence of light also resulted in an increased incidence of apoptosis and necrosis, albeit to a lower extent than in the presence of light. In general, treatment with nanoparticle-encapsulated drug(s) was more effective in inducing apoptosis/necrosis than treatment with drugs in solution.

We further confirmed enhanced induction of necrosis with combination therapy using fluorescence microscopy-based PI assay. Following light exposure, doxorubicin and methylene blue encapsulated in nanoparticles resulted in greater number of necrotic cells than that following any other treatment (Fig. 4). Phase contrast was used to confirm that approximately equal numbers of cells were present in all the treatment groups (not shown).

3.4. Cellular accumulation of doxorubicin

To determine the effect of combination therapy on cellular doxorubicin delivery, we compared the cellular levels of doxorubicin following treatment with combination therapy and that with doxorubicin alone (Fig. 5). Encapsulation of doxorubicin in nanoparticles had no significant effect on cellular accumulation of doxorubicin. Addition of verapamil, a P-gp inhibitor, resulted in a significant increase in cellular accumulation of doxorubicin ($P < 0.05$; ANOVA). Treatment with nanoparticle-encapsulated doxorubicin and methylene blue resulted in a significantly increased cellular accumulation of doxorubicin ($P < 0.05$). The relative enhancement in cellular accumulation of doxorubicin in the presence of methylene blue was comparable to that achieved in the presence of verapamil.

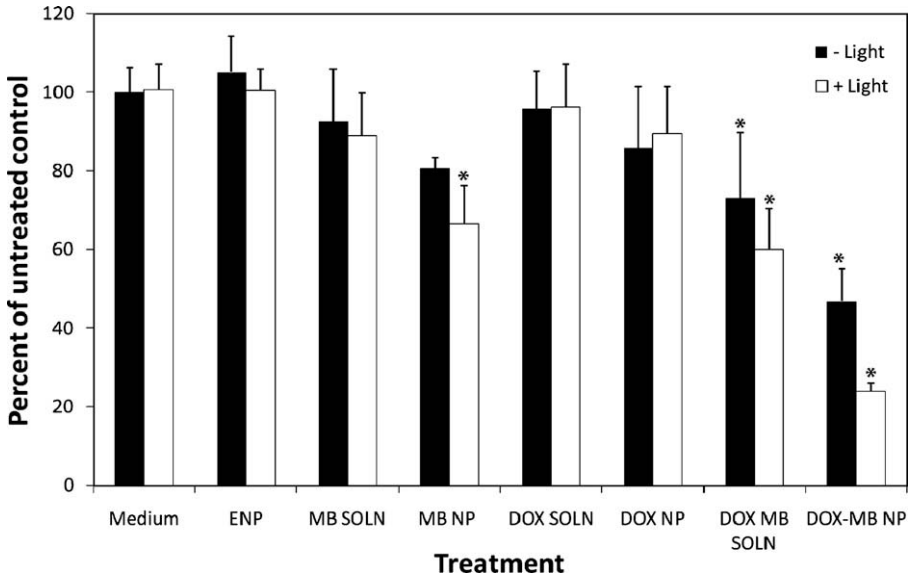

Fig. 3. Cytotoxicity following treatment of NCI/ADR-RES cells with combination PDT and chemotherapy. Cells were treated for 24 h with combination doxorubicin and methylene blue, either free (MB DOX solution) or encapsulated in nanoparticles (MB DOX NP). Some of the groups were exposed to light (+light) while others were used as dark controls. Cells incubated for 24 h with growth medium (medium), blank nanoparticles (ENP), methylene blue in solution (MB Solution), methylene blue loaded nanoparticles (MB NP), doxorubicin in solution (DOX solution), or doxorubicin in nanoparticles (DOX NP) with or without light exposure were used as control groups. Cell viability was quantified using MTS assay. Data as mean ± SD ($n = 8$). $^{*}P < 0.05$, ANOVA.

Table 1
Induction of apoptosis and necrosis determined by annexin-V/PI assay

Treatment	% Annexin-V^{+}	% PI^{+}	% Annexin-V^{+}/PI^{+}	Total
Methylene blue doxorubicin nanoparticles + light	3.82	16.76	25.04	45.62
Methylene blue nanoparticles + light	2.01	15.2	11.14	28.35
Methylene blue doxorubicin solution + light	6.31	7.96	19.8	34.07
Doxorubicin nanoparticles + light	3.92	7.95	12.72	24.59
Empty nanoparticles + light	3.06	5.45	7.57	16.08
Medium + light	3.6	3.3	6.27	13.17
Methylene blue doxorubicin nanoparticles	1.72	19.27	17.89	38.88
Methylene blue nanoparticles	2.08	11.11	16.76	29.95
Methylene blue doxorubicin solution	2.67	16.98	16.1	35.75
Doxorubicin nanoparticles	4.31	9.54	13.98	27.83
Empty nanoparticles	1.66	5.22	7.79	14.67
Medium	3.35	3.75	8.34	15.44

3.5. Intracellular distribution of doxorubicin and methylene blue

We initially determined the sub-cellular localization of doxorubicin/methylene blue using fluorescence microscopy. Lysotracker Green® was used to stain lysosomal vesicles with green fluorescence and DAPI was used to stain nuclei with blue fluorescence. Treatment with nanoparticles resulted in greater accumulation of doxorubicin and methylene blue (red fluorescence) in the nucleus (Fig. 6B; methylene blue images not shown). Overlay of images captured using the DAPI filter with those captured using Cy3 filter (for doxorubicin) or Cy5 filter (for methylene blue) resulted in purple fluorescence in nanoparticle treatment group, indicating colocalization of doxorubicin and methylene blue in the nuclei. Treatment with the drugs in solution resulted in their accumulation mainly in the lysosomal vesicles. Overlay of images captured using the FITC filter with those captured using Cy3 filter (for doxorubicin) or Cy5 filter (for methylene blue) resulted in yellow fluorescence for solution treatment group, indicating colocalization of the drugs in lysosomal compartments (Fig. 6A, methylene blue images not shown).

We also quantified the nuclear accumulation of doxorubicin following treatment with the combination therapy. Treatment with the combination of doxorubicin and methylene blue in nanoparticles resulted in a significantly higher nuclear accumulation of doxorubicin than that with the free drugs ($P < 0.05$, Fig. 7).

3.6. Intracellular ROS production

We next determined the effect of combination therapy on intracellular ROS production. As can be seen from the number of green fluorescent cells in Fig. 8, treatment with nanoparticle-encapsulated drug combination along with light exposure resulted in ROS production in a significantly more number of cells than treatment with the free drugs. Treatment with methylene blue nanoparticles along with light exposure also resulted in the generation of cellular ROS which, however, was appreciably less than that with the combination therapy. Other treatments resulted in minimal green fluorescence, indicating low levels of cellular ROS. For the sake of brevity, bright field images of cells and dark controls are not shown.

4. Discussion

Drug-resistant cancer cells have well-developed cellular defense mechanisms that reduce the accumulation of anticancer drug at its intracellular site of action. Resistant tumor cells overexpress

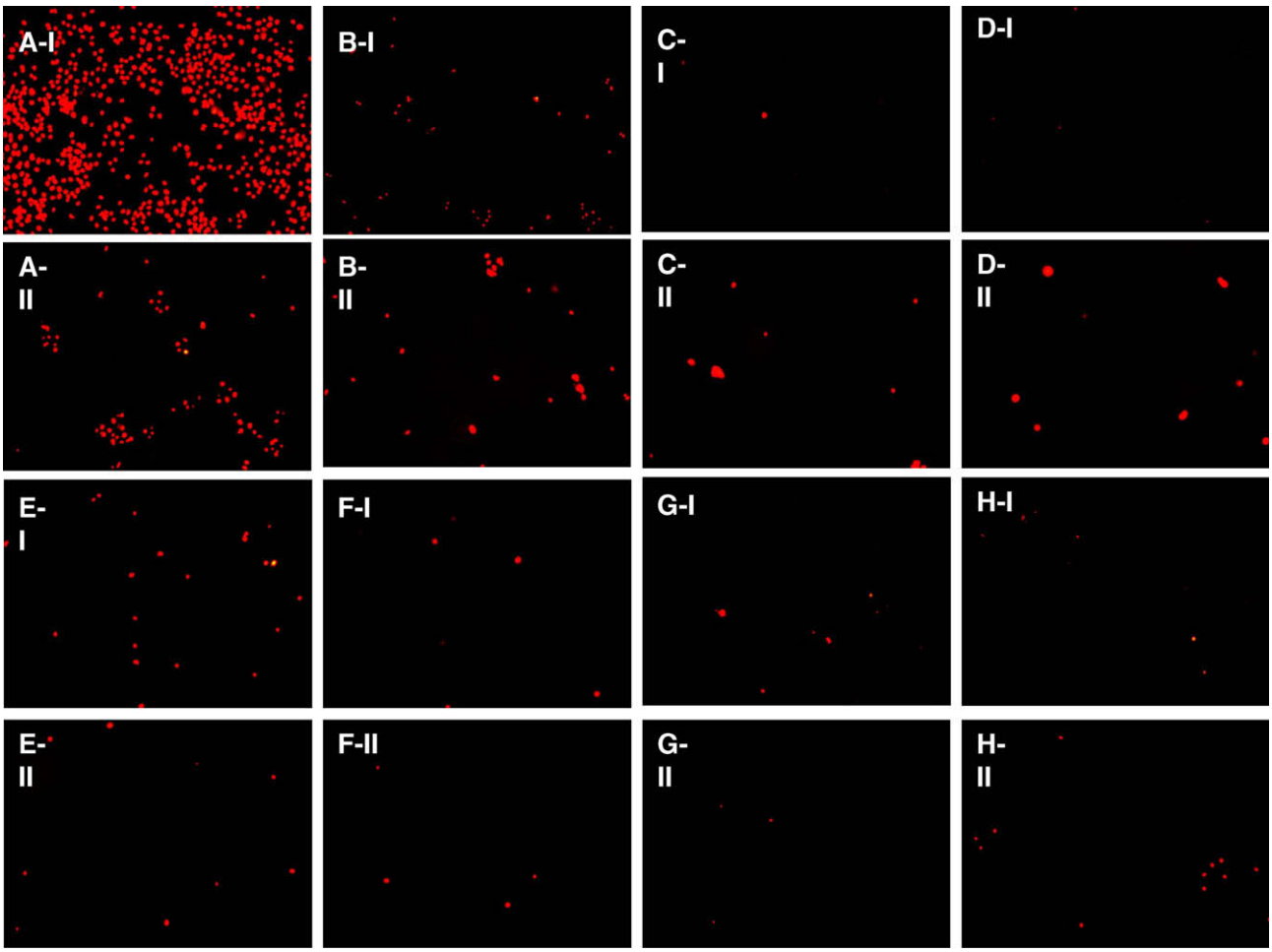

Fig. 4. Induction of necrosis following combination therapy. Cells were treated for 24 h with combination doxorubicin and methylene blue, either free (B) or encapsulated in nanoparticles (A). Some of the groups were exposed to light (groups I) at 2400 mJ/cm^2 while others were used as dark controls (groups II). Cells were incubated with PI and then imaged at 10× using a Cy3 filter. Cells incubated for 24 h with growth medium (H), blank nanoparticles (G), methylene blue in solution (F), methylene blue loaded nanoparticles (E), doxorubicin in solution (D), or doxorubicin in nanoparticles (C) were used as control groups.

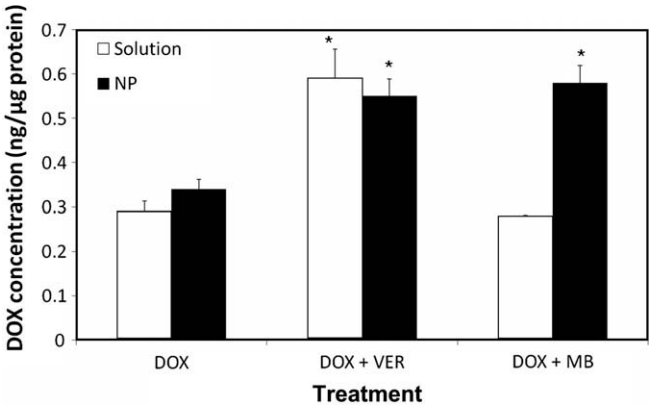

Fig. 5. Cellular accumulation of doxorubicin. Cells were incubated for 2 h with growth medium containing doxorubicin (DOX) and methylene blue (MB) in solution (solution) or encapsulated in nanoparticles (NP). Cells treated with doxorubicin in solution (DOX solution) or encapsulated in nanoparticles (DOX NP) with or without verapamil (VER) were used as control groups. Data as mean ± SD ($n = 6$). $^*P < 0.05$, ANOVA.

efflux transporters such as P-gp, which actively transport the drug out of the cell and reduce intracellular drug concentration [23,24]. Similarly, tumor cells can trap weak bases such as doxorubicin in acidic lysosomal vesicles, thereby reducing drug exposure to target organelle [3]. Acidic tumor microenvironment also plays a comparable role in tumor drug resistance [4].

Previous reports have shown that the use of combination PDT and chemotherapy results in enhanced cytotoxicity in drug-sensitive tumor cells [25,26]. Combining PDT using methylene blue, also a P-gp inhibitor [9], with chemotherapy is, thus, a potential approach to enhance cytotoxicity in drug-resistant tumor cells. Our previous studies have indicated that AOT-alginate nanoparticles are efficiently internalized into cells through endocytosis [18], and release the encapsulated drug slowly over a period of several days [18,22]. The fraction of methylene blue released from nanoparticles could inhibit P-gp mediated efflux of released doxorubicin; this in turn would improve intracellular doxorubicin accumulation in resistant tumor cells. Both released and nanoparticle-encapsulated methylene blue could participate in PDT-mediated ROS generation, because previous studies have demonstrated that the photosensitizer does not have to dissociate from the carrier for ROS production [27]. We hypothesized that increased doxorubicin availability inside the cells and light-induced ROS generation by methylene blue will result in enhanced cytotoxicity in drug-resistant tumor cells.

Previous studies have shown that NCI/ADR-RES cells overexpress P-gp and are highly resistant to anticancer drugs such as doxorubicin [28]. We observed a similar resistance in these cells

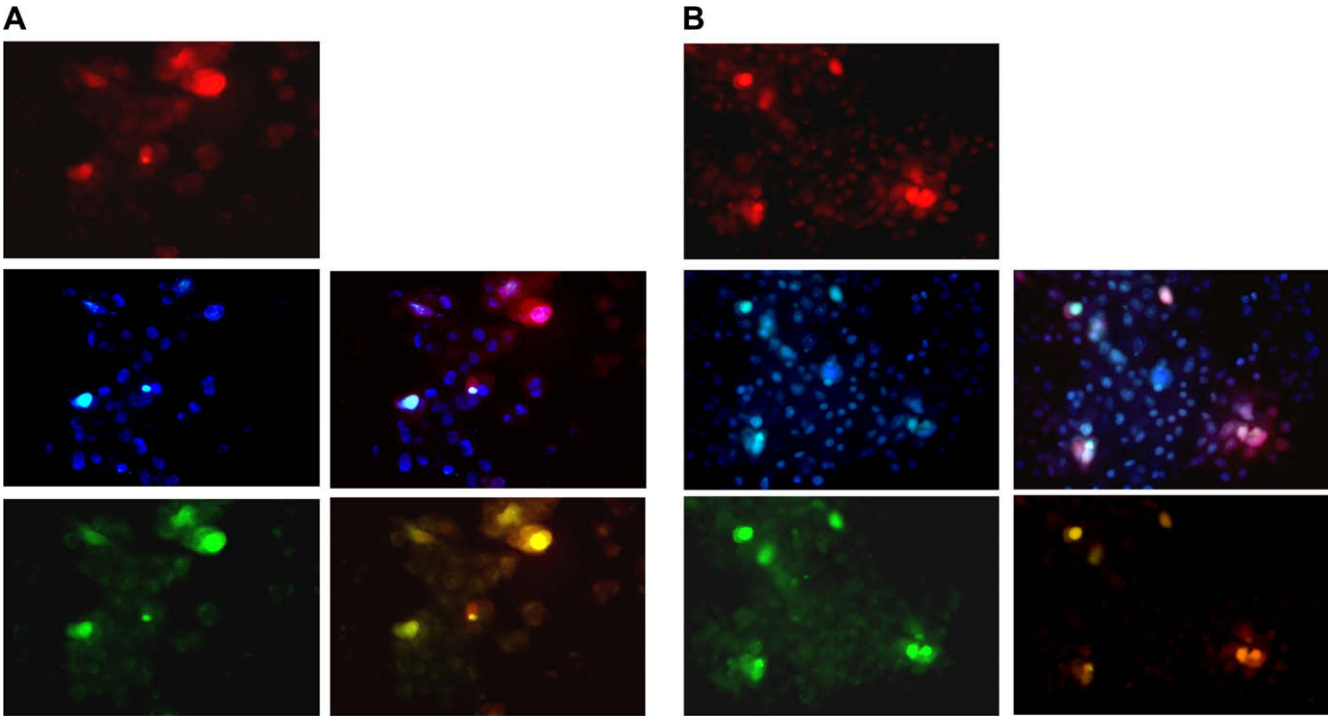

Fig. 6. Intracellular distribution of doxorubicin. Cells were treated with doxorubicin and methylene blue in solution (A) or in nanoparticles (B), and then counterstained with LysoTracker Green and DAPI. Images collected under Cy3 (red; for doxorubicin), FITC (green; for Lysotracker Green), and DAPI (blue; for DAPI) filters using a 10× objective were overlaid to determine the presence of doxorubicin in nucleus (indicated by purple fluorescence) or in lysosomes (yellow). (For interpretation of color mentioned in this figure the reader is referred to the web version of the article.)

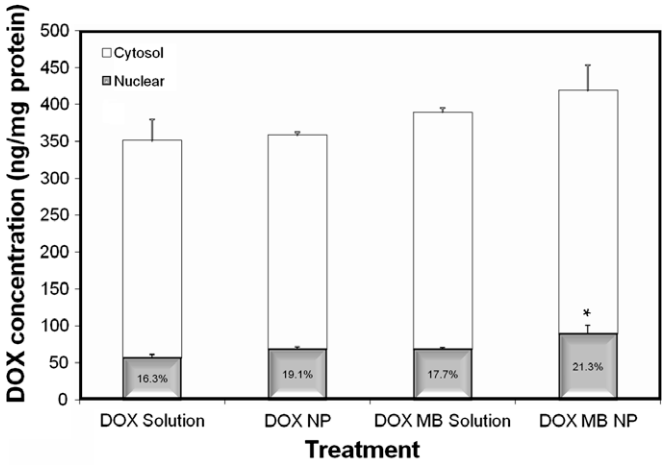

Fig. 7. Nuclear accumulation of doxorubicin. Cells were incubated for 2 h with growth medium containing methylene blue and doxorubicin in solution (DOX MB solution) or encapsulated in nanoparticles (DOX MB NP). Cells were fractionated and doxorubicin concentration in nuclear/cytosol fractions was quantified using HPLC. Cells incubated with doxorubicin in solution (DOX solution) or encapsulated in nanoparticles (DOX NP) were used as control groups. Data as mean ± SD ($n = 3$). $^{*}P < 0.05$, t-test.

to doxorubicin-induced cytotoxicity, irrespective of whether the drug was free or encapsulated in nanoparticles. While PDT with methylene blue (monotherapy) resulted in some cytotoxicity, maximum cell kill (~75%) was observed with the combination therapy (Fig. 3). To clarify the mechanism of cell death, we determined the induction of apoptosis and necrosis following combination therapy. Doxorubicin can induce apoptosis in tumor cells through multiple mechanisms, including DNA intercalation and inhibition of topoisomerase II [29]. PDT results in DNA and mitochondrial damage, resulting in the induction of apoptosis and/or necrosis [30,31]. The combination treatment resulted in a significant induction of both apoptosis and necrosis. The fact that we observed annexin-V^-/PI^+ cells in addition to annexin-V^+/PI^+ cells suggests that necrosis observed following combination therapy was independent of apoptosis. Since previous reports have shown that doxorubicin can induce G_2 arrest [32] and PDT with certain photosensitizers can result in G_0/G_1 arrest [33], we determined the effect of combination therapy on cell cycle. No significant differences were observed between treatment and control groups in the time-period studied (3 and 36 h post-PDT; data not shown). This suggests that the effect of combination therapy on cell viability was mainly through cell kill and not through cell cycle inhibition.

Although significant cytotoxicity was observed with the combination therapy in the absence of light, maximum cell kill was observed when the cells were exposed to light following the combination treatment (Fig. 3). This suggests that the photodynamic effect is required to maximize combination therapy-induced cytotoxicity. To further probe the role of the photodynamic effect, we determined intracellular ROS generation following treatment with combination therapy. ROS formation is considered the major mechanism of cytotoxicity in PDT [7]. Interestingly, light-activated combination treatment resulted in greater ROS production compared to light-activated methylene blue treatment (Fig. 8). While the reason for this enhanced ROS production is not clear, previous reports have shown that doxorubicin can also stimulate intracellular ROS production at supra-therapeutic concentrations [29]. It is possible that increased doxorubicin delivery to cells (see below) could have contributed to increased ROS production observed with combination therapy. On the other hand, the presence of doxorubicin in the same formulation can be expected to alter the microenvironment of methylene blue, and this can also influence the ROS yield significantly [34,35].

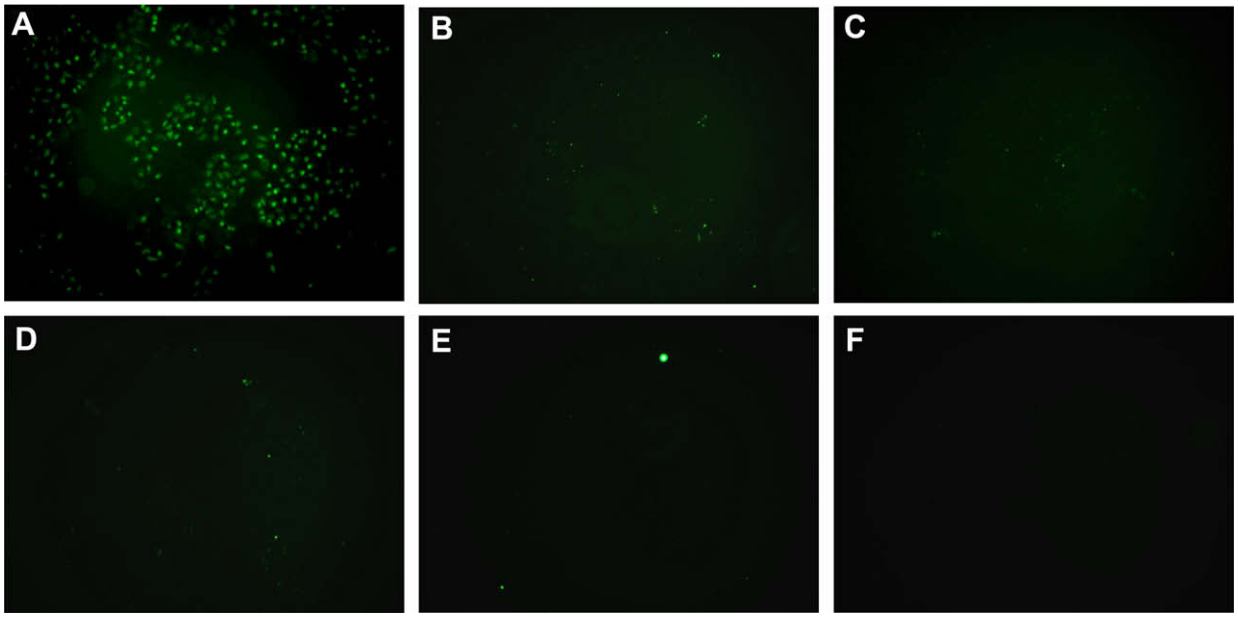

Fig. 8. Intracellular ROS production following combination PDT and chemotherapy. Cells were treated for 24 h with methylene blue and doxorubicin combination, either in solution (B) or encapsulated in nanoparticles (A). Cells were then incubated with 5 μM CM-H_2DCFDA for 1 h and some groups were exposed to light (2400 mJ/cm^2, 665 nm) while others were used as dark controls (data for dark controls not shown). Cells were then visualized under bright field and epi-fluorescence modes using a 10× objective. Cells incubated with growth medium (F), blank nanoparticles (E), methylene blue loaded nanoparticles (C), or doxorubicin in nanoparticles (D) were used as control groups.

The fact that significant cell kill was observed with combination nanoparticles even in the absence of light suggests that methylene blue contributes to enhanced cytotoxicity through mechanisms other than its photosensitization effect. *In vitro* release studies indicate that about 12–23% of encapsulated drugs were released in the time frame of the cytotoxicity study (24 h). While the actual fraction of the drug released inside the cells could be different from what was observed *in vitro*, the release study supports the notion that at least some of the encapsulated methylene blue is released from nanoparticles and can participate in the inhibition of P-gp mediated drug efflux. To further verify the role of methylene blue in P-gp inhibition, we determined the cellular accumulation of doxorubicin following treatment with doxorubicin and methylene blue. Combination treatment significantly enhanced the cellular accumulation of doxorubicin (Fig. 5). The extent of enhanced cellular levels of doxorubicin was comparable to that observed following treatment with combination of doxorubicin and verapamil, a P-gp inhibitor. Similar effects on doxorubicin's cellular accumulation and efficacy in drug-resistant cell lines have been previously reported for other P-gp inhibitors [36–38]. Soma et al. have reported that encapsulation of cyclosporine A, a P-gp inhibitor, along with doxorubicin in polyalkylcyanoacrylate nanoparticles reversed drug resistance *in vitro* [39]. It is also important to note that encapsulation of the drug in specific delivery systems such as polyalkylcyanoacrylate nanoparticles [40] or in AOT-alginate nanoparticles (at nanoparticle doses > 200 μg/ml) can overcome P-gp mediated drug efflux even in the absence of P-gp inhibitors [38].

Previous reports have shown that the intracellular location of the photosensitizer can significantly affect the therapeutic outcome of PDT [41]. Similarly, intracellular distribution of anticancer drugs such as doxorubicin can influence therapeutic efficacy [42]. Doxorubicin and methylene blue are weak bases that, after diffusing through the cell membrane, get trapped in acidic compartments like lysosomes, because of protonation in acidic pH [3]. Microscopic and quantitative studies demonstrate enhanced nuclear delivery of both drugs following encapsulation in nanoparticles (Figs. 6 and 7). Increased nuclear accumulation of doxorubicin confirms the potential of combination therapy to overcome resistance mechanisms that seek to reduce drug accumulation in target organelles. We speculate that enhanced methylene blue accumulation in the nucleus could have resulted in acute DNA damage following light exposure, which in turn, could have resulted in increased necrosis observed with the combination therapy. This notion is supported by our previous work [43], in which we demonstrated that AOT-alginate nanoparticles enhanced the nuclear delivery of methylene blue in drug-sensitive tumor cells.

To summarize, nanoparticle-mediated combination chemotherapy and PDT using doxorubicin and methylene blue resulted in improved cytotoxicity in drug-resistant tumor cells. Increased cellular and nuclear accumulation of the two drugs and enhanced intracellular ROS production appear to have contributed to the superior cytotoxicity observed with the combination therapy. In future studies, we plan to examine the involvement of different cell death pathways that may be evoked following combination therapy and the efficacy of the combination therapy in animal models of drug-resistant cancer.

Acknowledgement

Funding from Presidential Research Enhancement Program, Wayne State University is greatly acknowledged.

References

[1] J.A. Shabbits, R. Krishna, L.D. Mayer, Molecular and pharmacological strategies to overcome multidrug resistance, Expert. Rev. Anticancer Ther. 1 (2001) 585–594.
[2] G.D. Leonard, T. Fojo, S.E. Bates, The role of ABC transporters in clinical practice, Oncologist 8 (2003) 411–424.
[3] A.M. Kaufmann, J.P. Krise, Lysosomal sequestration of amine-containing drugs: analysis and therapeutic implications, J. Pharm. Sci. 96 (2007) 729–746.
[4] O. Alabaster, T. Woods, V. Ortiz-Sanchez, S. Jahangeer, Influence of microenvironmental pH on adriamycin resistance, Cancer Res. 49 (1989) 5638–5643.
[5] T.J. Dougherty, C.J. Gomer, B.W. Henderson, G. Jori, D. Kessel, M. Korbelik, J. Moan, Q. Peng, Photodynamic therapy, J. Natl. Cancer Inst. 90 (1998) 889–905.
[6] S.B. Brown, E.A. Brown, I. Walker, The present and future role of photodynamic therapy in cancer treatment, Lancet Oncol. 5 (2004) 497–508.

[7] H. An, J. Xie, J. Zhao, Z. Li, Photogeneration of free radicals (*OH and HB*-) and singlet oxygen (1O2) by hypocrellin B in TX-100 micelles microsurroundings, Free Radic. Res. 37 (2003) 1107–1112.
[8] I. Diamond, S.G. Granelli, A.F. McDonagh, S. Nielsen, C.B. Wilson, R. Jaenicke, Photodynamic therapy of malignant tumours, Lancet 2 (1972) 1175–1177.
[9] G.S. Trindade, S.L. Farias, V.M. Rumjanek, M.A. Capella, Methylene blue reverts multidrug resistance: sensitivity of multidrug resistant cells to this dye and its photodynamic action, Cancer Lett. 151 (2000) 161–167.
[10] P.J. Lou, P.S. Lai, M.J. Shieh, A.J. Macrobert, K. Berg, S.G. Bown, Reversal of doxorubicin resistance in breast cancer cells by photochemical internalization, Int. J. Cancer 119 (2006) 2692–2698.
[11] K. Berg, A. Dietze, O. Kaalhus, A. Hogset, Site-specific drug delivery by photochemical internalization enhances the antitumor effect of bleomycin, Clin. Cancer Res. 11 (2005) 8476–8485.
[12] M. Zeisser-Labouë be, A. Vargas, F. Delie, in: C.S. Kumar (Ed.), Nanoparticles for Photodynamic Therapy of Cancer, Nanomaterials for Cancer Therapy, vol. 1, Wiley-VCH, 2006, pp. 40–86 (Chapter 2).
[13] A. Vargas, M. Eid, M. Fanchaouy, R. Gurny, F. Delie, In vivo photodynamic activity of photosensitizer-loaded nanoparticles: formulation properties administration parameters and biological issues involved in PDT outcome, Eur. J. Pharm. Biopharm. 69 (2008) 43–53.
[14] I. Roy, T.Y. Ohulchanskyy, H.E. Pudavar, E.J. Bergey, A.R. Oseroff, J. Morgan, T.J. Dougherty, P.N. Prasad, Ceramic-based nanoparticles entrapping water-insoluble photosensitizing anticancer drugs: a novel drug-carrier system for photodynamic therapy, J. Am. Chem. Soc. 125 (2003) 7860–7865.
[15] L. Barraud, P. Merle, E. Soma, L. Lefrancois, S. Guerret, M. Chevallier, C. Dubernet, P. Couvreur, C. Trepo, L. Vitvitski, Increase of doxorubicin sensitivity by doxorubicin-loading into nanoparticles for hepatocellular carcinoma cells in vitro and in vivo, J. Hepatol. 42 (2005) 736–743.
[16] T. Betancourt, B. Brown, L. Brannon-Peppas, Doxorubicin-loaded PLGA nanoparticles by nanoprecipitation: preparation characterization and in vitro evaluation, Nanomedicine 2 (2007) 219–232.
[17] J.M. Koziara, T.R. Whisman, M.T. Tseng, R.J. Mumper, In-vivo efficacy of novel paclitaxel nanoparticles in paclitaxel-resistant human colorectal tumors, J. Control. Release 112 (2006) 312–319.
[18] M.D. Chavanpatil, A. Khdair, J. Panyam, Surfactant-polymer nanoparticles: a novel platform for sustained and enhanced cellular delivery of water-soluble molecules, Pharm. Res. 24 (2007) 803–810.
[19] H.A.F.R.G. Kelly, E.R. Jolly, P.A. Tove, The Pharmacokinetics and Metabolism of Dioctyl Sodium Sulfo-Succinate in Several Animal Species and Man, Report Submitted to WHO, Lederle Laboratories, American Cyanamid, 1973.
[20] S. Shiraishi, T. Imai, M. Otagiri, Controlled-release preparation of indomethacin using calcium alginate gel, Biol. Pharm. Bull. 16 (1993) 1164–1168.
[21] E. Tziampazis, A. Sambanis, Tissue engineering of a bioartificial pancreas: modeling the cell environment and device function, Biotechnol. Prog. 11 (1995) 115–126.
[22] M.D. Chavanpatil, A. Khdair, Y. Patil, H. Handa, G. Mao, J. Panyam, Polymer-surfactant nanoparticles for sustained release of water-soluble drugs, J. Pharm. Sci. 96 (2007) 3379–3389.
[23] G.D. Kruh, L.J. Goldstein, Doxorubicin and multidrug resistance, Curr. Opin. Oncol. 5 (1993) 1029–1034.
[24] Y. Ren, D. Wei, X. Zhan, Inhibition of P-glycoprotein and increasing of drug-sensitivity of a human carcinoma cell line (KB-A-1) by an antisense oligodeoxynucleotide–doxorubicin conjugate in vitro, Biotechnol. Appl. Biochem. 41 (2005) 137–143.
[25] E. Crescenzi, L. Varriale, M. Iovino, A. Chiaviello, B.M. Veneziani, G. Palumbo, Photodynamic therapy with indocyanine green complements and enhances low-dose cisplatin cytotoxicity in MCF-7 breast cancer cells, Mol. Cancer Ther. 3 (2004) 537–544.
[26] A. Zimmermann, H. Walt, U. Haller, P. Baas, S.D. Klein, Effects of chlorin-mediated photodynamic therapy combined with fluoropyrimidines in vitro and in a patient, Cancer Chemother. Pharmacol. 51 (2003) 147–154.
[27] W. Tang, H. Xu, R. Kopelman, M.A. Philbert, Photodynamic characterization and in vitro application of methylene blue-containing nanoparticle platforms, Photochem. Photobiol. 81 (2005) 242–249.
[28] M. Liscovitch, D. Ravid, A case study in misidentification of cancer cell lines: MCF-7/AdrR cells (re-designated NCI/ADR-RES) are derived from OVCAR-8 human ovarian carcinoma cells, Cancer Lett. 245 (2007) 350–352.
[29] G. Minotti, P. Menna, E. Salvatorelli, G. Cairo, L. Gianni, Anthracyclines: molecular advances and pharmacologic developments in antitumor activity and cardiotoxicity, Pharmacol. Rev. 56 (2004) 185–229.
[30] K. Plaetzer, T. Kiesslich, B. Krammer, P. Hammerl, Characterization of the cell death modes and the associated changes in cellular energy supply in response to AlPcS4-PDT, Photochem. Photobiol. Sci. 1 (2002) 172–177.
[31] R.D. Almeida, B.J. Manadas, A.P. Carvalho, C.B. Duarte, Intracellular signaling mechanisms in photodynamic therapy, Biochim. Biophys. Acta 1704 (2004) 59–86.
[32] W.Y. Siu, C.H. Yam, R.Y. Poon, G1 versus G2 cell cycle arrest after adriamycin-induced damage in mouse Swiss3T3 cells, FEBS Lett. 461 (1999) 299–305.
[33] C.M. Au, S.K. Luk, C.J. Jackson, H.K. Ng, C.M. Yow, S.S. To, Differential effects of, photofrin 5-aminolevulinic acid and calphostin C on glioma cells, J. Photochem. Photobiol. B 85 (2006) 92–101.
[34] Y. Vakrat-Haglili, L. Weiner, V. Brumfeld, A. Brandis, Y. Salomon, B. McLlroy, B.C. Wilson, A. Pawlak, M. Rozanowska, T. Sarna, A. Scherz, The microenvironment effect on the generation of reactive oxygen species by Pd-bacteriopheophorbide, J. Am. Chem. Soc. 127 (2005) 6487–6497.
[35] I. Bronshtein, K.M. Smith, B. Ehrenberg, The effect of pH on the topography of porphyrins in lipid membranes, Photochem. Photobiol. 81 (2005) 446–451.
[36] L. Bazargan, S. Fouladdel, A. Shafiee, M. Amini, S.M. Ghaffari, E. Azizi, Evaluation of anticancer effects of newly synthesized dihydropyridine derivatives in comparison to verapamil and doxorubicin on T47D parental and resistant cell lines in vitro, Cell Biol. Toxicol. 24 (2008) 165–174.
[37] W.G. Harker, D. Bauer, B.B. Etiz, R.A. Newman, B.I. Sikic, Verapamil-mediated sensitization of doxorubicin-selected pleiotropic resistance in human sarcoma cells: selectivity for drugs which produce DNA scission, Cancer Res. 46 (1986) 2369–2373.
[38] M.D. Chavanpatil, A. Khdair, B. Gerard, C. Bachmeier, D.W. Miller, M.P. Shekhar, J. Panyam, Surfactant-polymer nanoparticles overcome P-glycoprotein-mediated drug efflux, Mol. Pharm. 4 (2007) 730–738.
[39] C.E. Soma, C. Dubernet, D. Bentolila, S. Benita, P. Couvreur, Reversion of multidrug resistance by co-encapsulation of doxorubicin and cyclosporin A in polyalkylcyanoacrylate nanoparticles, Biomaterials 21 (2000) 1–7.
[40] A.C. de Verdiere, C. Dubernet, F. Nemati, E. Soma, M. Appel, J. Ferte, S. Bernard, F. Puisieux, P. Couvreur, Reversion of multidrug resistance with polyalkylcyanoacrylate nanoparticles: towards a mechanism of action, Br. J. Cancer 76 (1997) 198–205.
[41] I. Walker, S.A. Gorman, R.D. Cox, D.I. Vernon, J. Griffiths, S.B. Brown, A comparative analysis of phenothiazinium salts for the photosensitisation of murine fibrosarcoma (RIF-1) cells in vitro, Photochem. Photobiol. Sci. 3 (2004) 653–659.
[42] D. Goren, A.T. Horowitz, D. Tzemach, M. Tarshish, S. Zalipsky, A. Gabizon, Nuclear delivery of doxorubicin via folate-targeted liposomes with bypass of multidrug-resistance efflux pump, Clin. Cancer Res. 6 (2000) 1949–1957.
[43] A. Khdair, B. Gerard, H. Handa, G. Mao, M.P. Shekhar, J. Panyam, Surfactant-Polymer Nanoparticles Enhance the Effectiveness of Anticancer Photodynamic Therapy, Mol. Pharm., (2008), in press, doi: 10.1021/mp800026t (Epub ahead of print).